

Formation and evolution of water menisci in unsaturated granular media

S. D. N. LOURENÇO*, D. GALLIPOLI†, C. E. AUGARDE*, D. G. TOLL‡, P. C. FISHER* and A. CONGREVE§

Loose particles in moist granular materials, such as unsaturated soils, are held together by capillary forces acting at the interparticle contacts. The magnitude of these capillary forces depends on the surface tension and on the radius of curvature of the menisci, which in turn depends on the contact angle of the air/water interface against the surface of the solid particles. Menisci are usually assumed to be predominantly concave on the side of the air with negative water pressure (relative to the atmosphere). Evidence for this comes from direct observations at the millimetre scale or from theoretical assumptions. This note presents data from environmental scanning electron microscopy of particles at the micrometre scale that contradict this assumption and show for the first time that, for a given water content, the contact angle between air/water interfaces and grains can give rise to a variety of meniscus shapes, with curvatures not all concave on the side of air. It was found that the curvature of water menisci, in both idealised and natural granular materials with variable particle sizes, shapes and nature, could vary along the border of a single meniscus or differ from one point to another separated at the micrometre scale, and is also dependent on the nature of materials and wetting history. Menisci can have both predominantly convex shapes (corresponding to compressive capillary pressure) and predominantly concave shapes (corresponding to tensile capillary water pressure). These observations confirm the importance of surface tension in the air/water interfaces (often also referred to as ‘contractile skin’) in holding particles together.

KEYWORDS: microscopy; partial saturation; suction

La cohésion entre particules lâches dans des matières granulaires humides, par exemple des sols non saturés, est assurée par des forces capillaires agissant sur les points de contact inter-particules. La magnitude de ces forces capillaires est fonction de la tension superficielle et du rayon de courbure des ménisques, qui sont, à leur tour, tributaires de l’angle de contact de l’interface air/eau contre la surface des particules solides. On suppose généralement que les ménisques sont principalement concaves du côté de l’air à pression négative de l’eau (relativement à l’atmosphère). Ceci a été démontré par des observations directes à l’échelle millimétrique, ou par des hypothèses théoriques. Cette communication présente des données obtenues par la microscopie électronique de scannage environnementale de particules à l’échelle micrométrique, qui contredisent cette hypothèse, et montrent, pour la première fois, que pour une certaine teneur en eau, l’angle de contact entre les interfaces air/eau et les grains peut donner lieu à une série de formes de ménisques, avec des courbures qui ne sont pas toutes concaves sur le côté de l’air. On a relevé que la courbure des ménisques d’eau, dans des matières granulaires idéalisées et naturelles à granulométrie, forme et nature variables sont susceptibles de varier le long de la limite d’un ménisque unique, ou se distingue d’un point à un autre, séparés à l’échelle micrométrique, et est également tributaire de la nature des matières et de l’historique du mouillage. Les ménisques peuvent présenter à la fois des formes principalement convexes (correspondant à la pression capillaire en compression) et principalement concaves (correspondant à la pression capillaire de l’eau en tension). Ces observations confirment l’importance de la tension superficielle dans les interfaces air/eau (souvent dénommée «peau contractile») pour la cohésion des particules.

INTRODUCTION

Water capillarity regulates part of the intergranular bonding forces in unsaturated particle mixtures. These forces are exerted by water menisci located at the contact between particles, and depend on the average curvature, surface tension and contact angle of the menisci (Fisher, 1926). These stabilising forces lead to the visible phenomenon of steeply inclined free surfaces in particle piles, such as sandcastles, excavations, compacted earth constructions and silos (Vaughan & Walbancke, 1973; Fitzpatrick *et al.*, 2003; Jaquin *et al.*, 2009). The water menisci are usually assumed

to be either concave or convex for a given material (Fisher, 1926; Tuller *et al.*, 1999).

The term ‘capillarity’ is often used to lump together two distinct physical actions of menisci on solid grains: (a) the pressure exerted by water, which can be either compressive or tensile, and depends on the mean curvature of the meniscus; and (b) the pull exerted by the surface tension acting inside the air/water interface (often referred to as the ‘contractile skin’, e.g. Fredlund & Rahardjo, 1993). The mean curvature of the meniscus can be either positive or negative with respect to the air, corresponding to ‘predominantly concave’ or ‘predominantly convex’ shapes. The term ‘predominantly’ has been here introduced to indicate that the shape of the air/water interface is related to the mean curvature of the water meniscus, whose principal curvatures might also have opposite signs. If the meniscus is predominantly concave on the side of the air, the water pressure will be negative (tensile) with respect to the air pressure, whereas the opposite is true if the meniscus is predominantly convex.

Schematic representations of predominantly concave and convex menisci at the contact between two solid grains idealised as spheres are given in Figs 1(a) and 1(b) respec-

Manuscript received 1 April 2011; revised manuscript accepted 6 May 2011. Published online ahead of print 18 November 2011.

Discussion on this paper closes on 1 August 2012, for further details see p. ii.

* School of Earth and Ocean Sciences, Cardiff University, UK.

† School of Engineering, University of Glasgow, UK.

‡ School of Engineering and Computing Sciences, Durham University, UK.

§ Department of Chemistry, Durham University, UK.

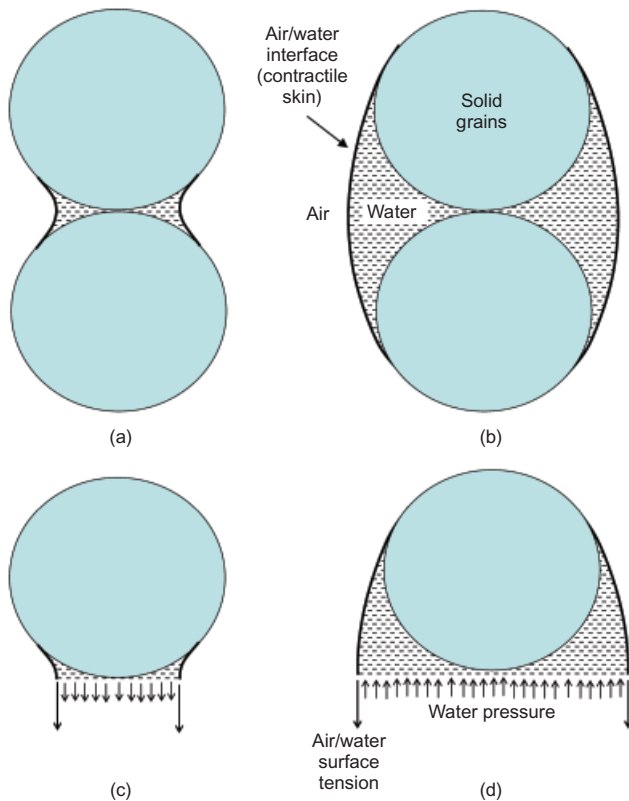


Fig. 1. Schematic representation of (a) predominantly concave meniscus and (b) predominantly convex meniscus located at contact between two solid grains idealised as spheres. Water pressure exerted on each solid grain is (c) tensile for predominantly concave meniscus and (d) compressive for predominantly convex meniscus; surface tension is always tensile

tively. In addition, Figs 1(c) and 1(d) show the forces exerted by both surface tension and water pressure for a predominantly concave and a predominantly convex meniscus respectively. In a predominantly concave meniscus the water pressure is tensile, and pulls the two grains together, as does the surface tension acting inside the contractile skin. In a predominantly convex meniscus the water pressure is instead compressive, and pushes the two grains away, while the surface tension acting inside the contractile skin pulls the grains together. Therefore the resultant force exerted on each grain by a predominantly convex meniscus can be compressive or tensile, depending on the relative magnitude of surface tension and water pressure.

The Young–Laplace equation is used to express the magnitude of the water pressure (u_w) inside the meniscus as

$$u_w = -2T \left(\frac{h_1 + h_2}{2} \right) \quad (1)$$

where h_1 and h_2 are the principal curvatures (i.e. the reciprocals of the principal radii of curvature) of the meniscus, and T is the air/water surface tension.

The mean curvature and surface tension of intergranular menisci will determine whether a pile of particles can support itself (Fisher, 1926; Israelachvili, 1991). Understanding the nature of curvature in intergranular menisci is of prime importance to fields that deal with strength and deformation of granular materials in an unsaturated condition, such as soil mechanics, soil science and powder technology, and has a variety of applications in the construction industry and ground engineering, the pharmaceutical and food industry, agriculture and mineral exploration.

The contact angle between the contractile skin and the solid grains is another important factor affecting the geometrical arrangement of water menisci at the particle contacts. The value of the contact angle depends on the menisci's movement (De Gennes, 1985), including their velocity (Hoffman, 1975), the presence of microasperities (Taniguchi & Belfort, 2002), super-hydrophobicity associated with the sub-millimetre surface topography (the lotus leaf effect; Bachmann & McHale, 2009), the presence of impurities and deposition of solutes (Fisher & Israelachvili, 1981), organic matter (Chenu *et al.*, 2000), microbial cells (Busscher *et al.*, 2000), and the type of soil and minerals (Table 1). At the same time, the presence of surfactants affects the value of surface tension acting inside the contractile skin (Karagunduz *et al.*, 2001).

Previous attempts to observe the formation and evolution of water menisci have been limited to scales some orders of magnitude larger than the size of natural soil particles, such as mixtures of water, air and small glass beads (Sjöblom, 2000; Reinson *et al.*, 2005). Correlation of these findings with real soils is clearly difficult, owing to the relatively large size of the particles used. This note presents and discusses observations of artificial unsaturated granular materials, consisting of very small spheres close to the scale of natural granular soils, and observations of unsaturated natural soils themselves.

MATERIALS AND METHODS

The environmental scanning electron microscope (ESEM) enables moist materials to be viewed without pre-treatment, at dimensions from millimetres down to micrometres. Condensation or evaporation of water can be controlled by varying the vapour pressure and temperature in the ESEM chamber. The ESEM has previously been used to observe water menisci in different conditions: at the contact of a cantilever tip of an atomic force microscope and a flat substrate (Weeks *et al.*, 2005); in monosized silica spheres arranged in a single layer (Lampenschurf *et al.*, 2000); in reservoir rocks (Buckman *et al.*, 2000; Skauge *et al.*, 2006) and chalk (Sorgi & De Gennaro, 2007), and in bentonite MX80 and kaolin aggregates (Montes-H, 2005; Lourenço *et al.*, 2008). The instrument used in the present study is an FEI XL-30 field emission gun ESEM with a gaseous secondary electron detector and equipped with a Peltier stage for controlling temperature. All tests in this study were conducted in the same ESEM model under the same conditions at three different locations (Cardiff, Durham and Heriot-Watt universities).

Details of the materials used in this study are given in Table 2. These include microspheres made of silica (2 μm and 6 μm diameter) and five other natural granular materials of different types, particle sizes and shapes. The amine functionalised organosilica microspheres were synthesised at Durham University according to a method modified by Miller *et al.* (2005). The spheres were stored in deionised water. Menisci in unsaturated mixtures of these materials

Table 1. Contact angles of water menisci in soils and minerals

| Material | Contact angle |
|-------------|-------------------------------------|
| Sandy loam | 68.9° (Letley <i>et al.</i> , 1962) |
| Clayey soil | 65.2° (Letley <i>et al.</i> , 1962) |
| Quartz | 30° (Fisher & Lark, 1980) |
| Dolomite | 5.6–7.6° (Gence, 2006) |
| Mica | 10° (Bryant <i>et al.</i> , 2006) |

Table 2. Characteristics of the granular materials used in the study

| Material | Bulk composition* | Size: μm^\dagger | Shape [†] |
|-------------|--|-----------------------------|------------------------|
| Spheres | Organosilicates | 2 6 | Spherical Spherical |
| Sand A | Quartz | 100–300 | Sub-rounded |
| Sand B | Quartz | 200–300 | Sub-rounded |
| Clay A | Mixed phase with kaolinite, illite, montmorillonite, quartz, calcite | 1–10 | Platy to sub-rounded‡ |
| Sand C | Quartz | 200–300 | Sub-angular |
| London Clay | Mixed phase with illite, kaolinite, montmorillonite, quartz, gypsum | 1–10 | Platy to sub-rounded‡ |

* Reflects the overall composition of the sample rather than the spot being observed; obtained by X-ray diffraction.

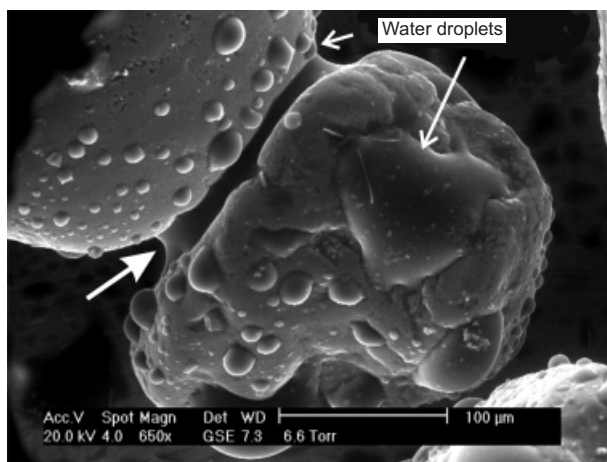
† As observed shape and size of the materials (as individual particles or in an aggregate form).

‡ Platy refers to individual clay particles, whereas sub-rounded refers to an aggregate of plates.

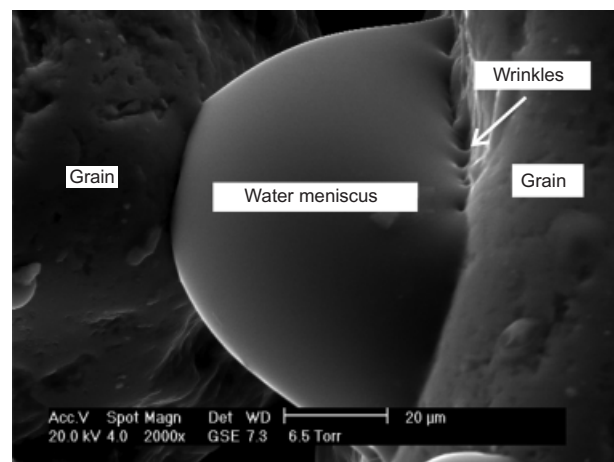
were directly observed by placing an aqueous solution of the material on the Peltier stage of the ESEM at a temperature of 5°C. The lower temperatures allow higher-quality imaging and follow the ESEM temperature settings by Weeks *et al.* (2005) and Sorgi & De Gennaro (2007). Particular care was taken to ensure that the grains did not pile up, in order to avoid temperature gradients (Lourenço *et al.*, 2008). This was achieved by preparing a well-diluted sample. In all images shown here (Figs 2–6) the particles rest directly on the substrate of the Peltier stage. The temperature was set constant at 5°C, while the vapour pressure was varied to induce evaporation or condensation of water. The tempera-

ture accuracy of the Peltier stage is $\pm 0.5^\circ\text{C}$. The materials were subjected to cycles of wetting and drying in which relative humidity was varied between 100% and a minimum of 35%.

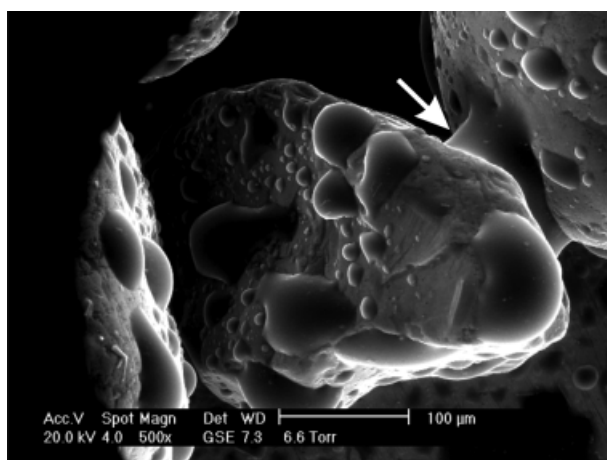
During all tests, a total of 835 still images (at 5100 dpi) were taken. A working distance of 7.5–10.5 mm was used inside the ESEM chamber, with an operating voltage of 20 kV, and spot size of 4. Under these conditions, it was possible to obtain images down to the nanoscale with up to 80 000 \times magnification. All images presented here are originals. The water vapour pressure is shown in torr units (1 Pa = 133.322 torr).



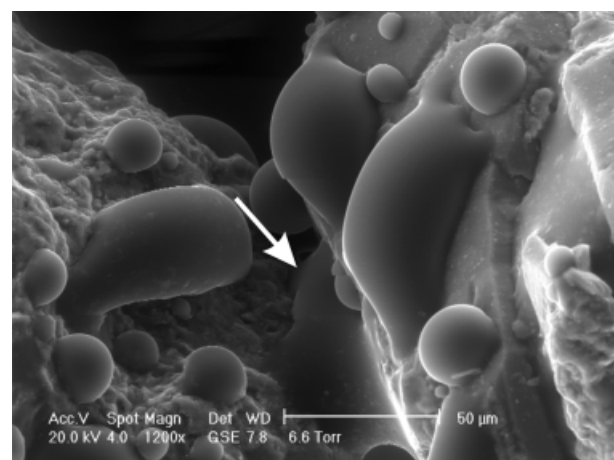
(a)



(b)



(c)



(d)

Fig. 2. Water menisci form at contacts of sand grains: (a), (c) and (d) show predominantly concave menisci; (b) shows predominantly convex menisci. The ‘wrinkles’ of the air/water interfaces are clear in (b) (bold arrows indicate water menisci at contacts with grains). Image settings (RH, material): (a) 100%, Sand B; (b) 99%, Sand B; (c) 100%, Sand B; (d) 100%, Sand C

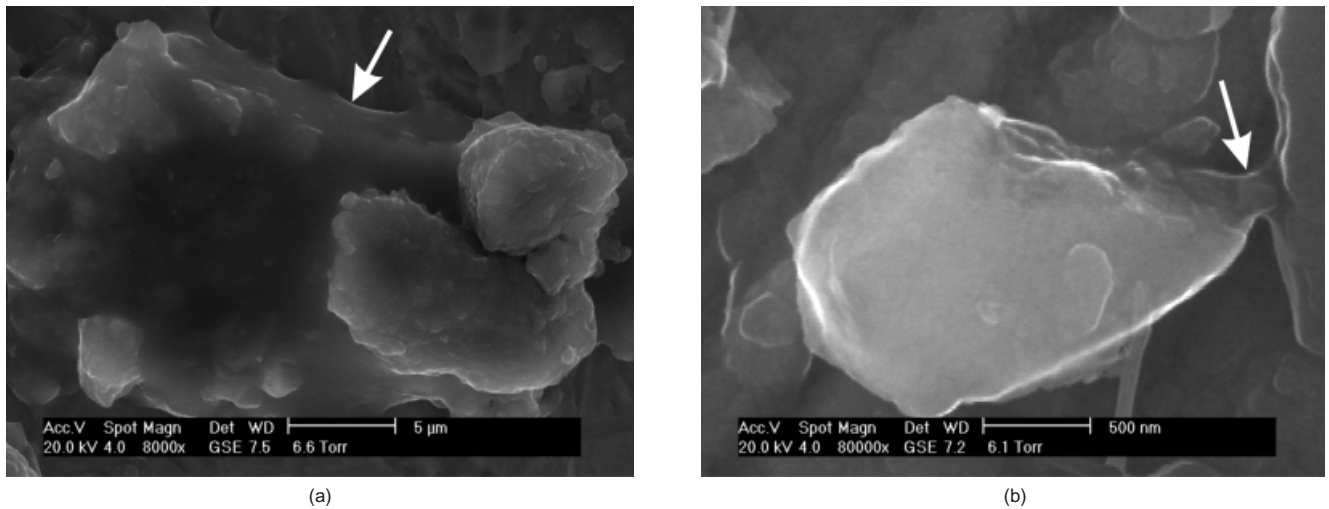


Fig. 3. Water menisci form at contacts of clay aggregates: (a), (b) show affinity of clays to water (bold arrows indicate water menisci at contacts between aggregates). Image settings (RH, material): (a) 100%, Clay A; (b) 93%, London Clay

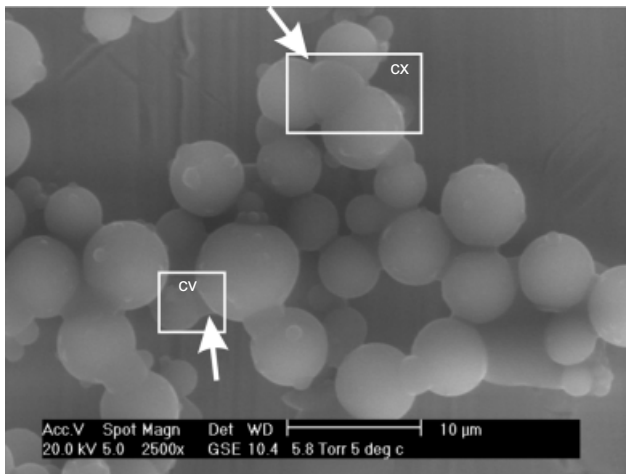


Fig. 4. Water menisci form at contacts of micrometre-sized spheres. Image shows concave (cv) and convex (cx) menisci coexisting at same relative humidity: image settings (RH): 88%

DYNAMIC ENVIRONMENTAL CONDITIONS

The images represent dynamic conditions where the snapshots were taken as the menisci changed in shape. This resembles real field conditions, where the menisci are continuously changing as a function of fluctuations in environmental conditions (e.g. humidity, temperature). The materials did not achieve true hydraulic equilibrium in the traditional unsaturated soils testing sense, where suction remains constant, owing to the impossibility of changing the water vapour pressure in steps lower than 0.1 torr (equivalent to $\sim 1.6\%$ step at a high relative humidity at 5°C). This meant that most condensation occurred when the relative humidity approached 100%. However, the menisci should not be considered transient (in a temporary condition), since the time-scales involved are relatively large (minutes), and nearer to those that pertain in nature: for instance, the relative humidity history for the image in Fig. 2(c) was 76% (2 min), 91% (2 min), 95% (2 min), 96% (2 min), 100% (4 min).

GENERAL WATER MENISCUS SHAPES

Water menisci can depart significantly from the often assumed predominantly concave shape (Fig. 2). The shapes

of menisci are controlled primarily by the nature of the materials involved, irrespective of the size and shape of the individual grains. Clays develop continuous films of water with a predominantly concave shape that completely wrap and bridge the aggregates (Fig. 3), whereas in all other materials the menisci show a mixture of predominantly concave and predominantly convex curvatures at the same relative humidity (Figs 1 and 4).

It is interesting to note that the above result seems to contradict equation (1), which postulates that, under equilibrium conditions at a given value of matric suction, the average meniscus curvature should be the same at any point over the air/water interface. In particular, if the osmotic component of suction is neglected so that total suction coincides with matric suction, each imposed value of relative humidity should generate the same meniscus curvature at all locations and for all material types according to equation (1). Further research is needed to understand the reasons of this apparent contradiction.

For the case of predominantly convex menisci, the contact angle also appears to vary along the border of the air/water interface, with the development of 'wrinkles' due to the unevenness of the solid particles (Figs 2(b) and 2(d)).

Some unique features of the meniscus evolution were identified when relative humidity was increased until the sample was flooded. Meniscus shape developed progressively at the interparticle contacts for the micron-sized silica spheres (Fig. 5), whereas for the sands (100 times larger in size) the menisci tended to grow by coalescing of droplets (Fig. 6). Observations also demonstrated that there is no preference for water to condense in small spaces (Israelachvili, 1991).

It is often assumed that the stabilising interparticle forces in unsaturated granular materials are generated mainly by the tensile water pressure acting inside concave menisci with low contact angles (soils are assumed wettable in soil mechanics) rather than by the surface tension acting in the contractile skin. The observation in this work of menisci having a predominantly convex shape suggests, however, that compressive water pressures, producing repulsive interparticle forces, can exist in unsaturated granular materials (Fig. 4(b)). In such circumstances, surface tension alone is responsible for pulling grains together. Therefore the force exerted by the contractile skin on solid grains plays an essential role in 'bonding' solid particles, so producing the cohesive strength and stiffness of unsaturated granular materials

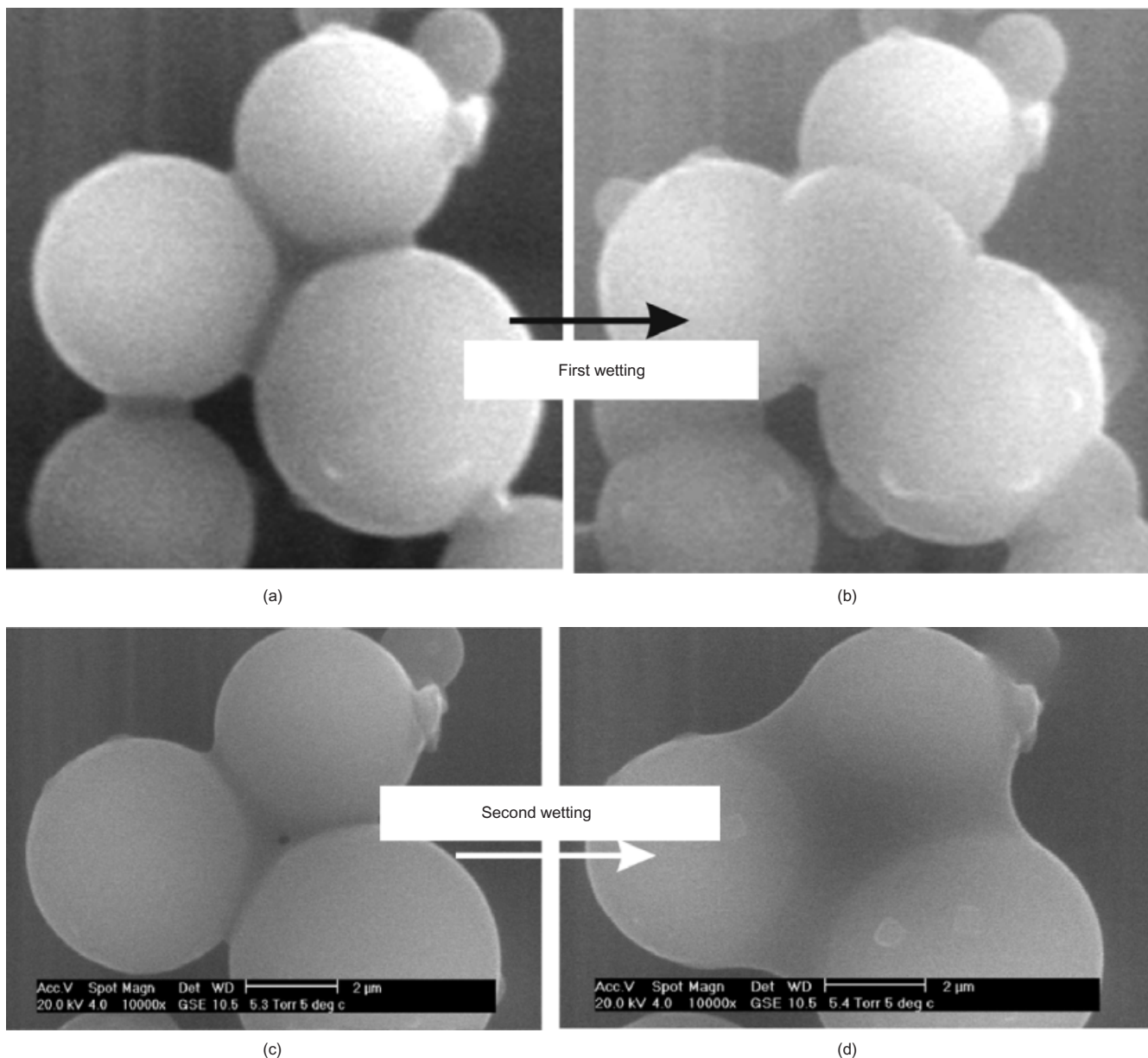


Fig. 5. Physical features of observed menisci in micrometre-sized spheres during first and second wetting: (a), (b) close-ups from rectangle with cx meniscus in Fig. 3 during first wetting, showing convex curvatures (contact angle $\sim 80^\circ$); (c), (d) meniscus concave curvatures during second wetting (contact angle $\sim 25^\circ$). Image settings (RH): (a) 82%; (b) 88%; (c) 81%; (d) 82%

(Gallipoli *et al.*, 2003). The relevance of surface tension has been already demonstrated. For example, Berney IV *et al.* (2003) revealed that the addition of anionic surfactants to water increases the dry density of compacted silty sands. This was attributed to a decrease in the surface tension of the air/water interface.

WATER MENISCUS SHAPES RESULTING FROM WETTING–DRYING CYCLES

The water menisci assumed predominantly concave curvatures in consecutive wetting paths: that is, in the wetting paths of successive drying–wetting cycles of the granular material (Fig. 5). This tendency is thought to reflect water adsorption to the particle surfaces by way of van der Waals forces, which causes the water to spread more easily, with a smaller contact angle, when condensing for a second time. This is consistent with previous measurements of contact angle of water droplets on a polyimide substrate that showed

decreasing advancing and receding angles during wetting–drying cycles (Hennig *et al.*, 2004).

The micrographs of sand grains reveal similar trends. A hydrophobic behaviour was observed when the material was wetted for the first time, with condensation of numerous meniscus domes of variable dimensions all around the surfaces (Fig. 6). On the other hand, during subsequent condensation–evaporation cycles, water tended to spread with greater ease and to develop predominantly concave menisci. The only difference from the experiments with the silica spheres was that, owing to the larger size of the sand grains, smaller menisci condensed at the interparticle contacts at similar values of relative humidity. These smaller menisci tended to grow and coalesce into larger menisci bridging the grains as the sample came to equilibrium under the imposed relative humidity (Figs 6(b) and 6(d)).

The above results are also consistent with field studies that show that the affinity of water to soil particles increases with water content (Doerr *et al.*, 2000).

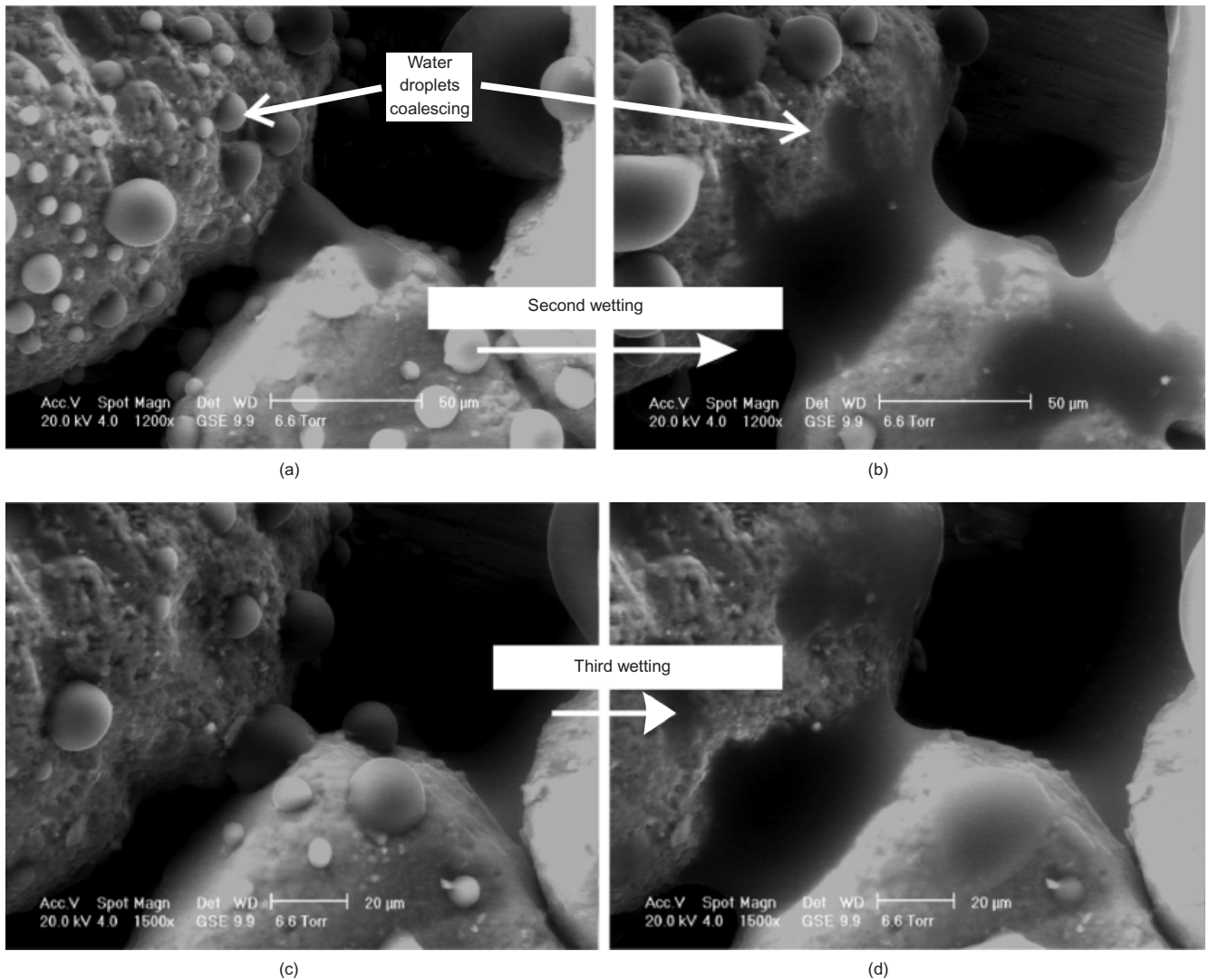


Fig. 6. Physical features of observed menisci in sand grains during second and third wettings: (a), (b) second wetting; (c), (d) third wetting (first wetting was observed in a different part of the sample). Image settings (RH, material): 100%, Sand A

CONCLUSIONS

This note presents observations of water menisci in granular materials at different relative humidities using the environmental scanning electron microscope (ESEM). The ESEM imposes a wet environment, corresponding to a given relative humidity, by controlling temperature and water vapour pressure, and can be used to perform wetting–drying cycles without removing the sample from the microscope chamber. The observations provide evidence at the micrometre scale of capillary effects previously observed at a scale $1000\times$ bigger. The key observations are as follows.

- Soils, in general, should not be assumed as wettable, and the images acquired during this work revealed contact angles higher than zero in several circumstances.
- For sands at high relative humidity, menisci increased in size in dome shapes until collapsing or coalescing to form a continuous liquid phase, whereas clays wet by a growing continuous film of water.
- Contact angles were found to vary with relative humidity cycles: that is, convex menisci were seen to develop in the first wetting, followed by concave menisci in a second wetting.
- Surface tension in the air/water interfaces could play a key role in pulling particles together by generating a

cohesive component of strength, even in the presence of positive water pressures inside the menisci.

- The use of the ESEM is confirmed as a powerful tool to study the behaviour of moist granular mixtures.

These findings promote further research to consider the influence of the contact angle and surface tension of water menisci on the hydromechanical behaviour of partially saturated granular materials. The importance of the contact angle is already recognised in soil science, but less so in unsaturated soil mechanics. As an example, these observations could be a starting point for the improvement of stress–strain models for the soil that take the water meniscus curvature into account (Gallipoli *et al.*, 2003; Wheeler *et al.*, 2003), the development of experimental techniques to test soils under hydrophobic conditions (e.g. measurement of positive water pressures in a hydrophobic soil), or to better understand the erosional and landsliding processes in burned slopes (Doerr *et al.*, 2000; Cannon *et al.*, 2010).

ACKNOWLEDGEMENTS

The authors thank Dr David Beamer (FEI Instruments), Ms Helen Riggs (Durham University) and Dr Jim Buckman (Heriot-Watt University) for the help provided with the ESEM work. Mr Anthony Oldroyd conducted the X-ray

diffraction in the clay samples. Professor Ian Hall (Cardiff University) is thanked for his constructive comments on an early draft of the manuscript. This research was partially supported by the Engineering and Physical Sciences Research Council (UK), Wykeham Farrance Division (Controls Testing SA) and the European Commission by way of the 'Marie Curie' Research Training Network, contract number MRTN-CT-2004-506861.

REFERENCES

- Bachmann, J. & McHale, G. (2009). Superwater repellent surfaces: a model approach to predict contact angle and surface energy of soil particles. *Eur. J. Soil Sci.* **60**, No. 3, 420–430.
- Berney IV, E. S., Peters, J. F., Newman, J. K. & Smith, D. M. (2003). Effect of surfactant on dry-side compaction of silty sand. *Transp. Res. Record* **1819B**, 57–62.
- Bryant, E. M., Bowman, R. S. & Buckley, J. S. (2006). Wetting alteration of mica surfaces with polyethoxylated amine surfactants. *J. Petrol. Sci. Engng* **52**, Nos 2–4, 244–252.
- Buckman, J. O., Todd, A. C. & Hill, P. I. (2000). Observations on a reservoir rock wettability using an environmental scanning electron microscope. *Microscopy and Analysis* **14**, No. 2, 35–37.
- Busscher, H. J., Weerkamp, A. H., van der Mei, H. C., van Pelt, A. W. J., De Jong, H. P. & Arends, J. (2000). Measurement of the surface free energy of bacterial cell surfaces and its relevance for adhesion. *Appl. Environ. Microbiol.* **48**, No. 5, 980–983.
- Cannon, S. H., Gartner, J. E., Rupert, M. G., Michael, J. A., Rea, A. H. & Parrett, C. (2010). Predicting the probability and volume of postwildfire debris flows in the intermountain western United States. *GSA Bulletin* **122**, Nos 1–2, 127–144.
- Chenu, C., Bissonnais, Y. L. & Arrouays, D. (2000). Organic matter influence on clay wettability and soil aggregate stability. *Soil Sci. Soc. Am. J.* **64**, No. 4, 1479–1486.
- De Gennes, P. G. (1985). Wetting: statics and dynamics. *Rev. Modern Phys.* **57**, 3, 827–863.
- Doerr, S. H., Shakesby, R. A. & Walsh, R. P. D. (2000). Soil water repellency: its causes, characteristics and hydro-geomorphological significance. *Earth Sci. Rev.* **51**, Nos 1–4, 33–65.
- Fisher, R. A. (1926). On the capillary forces in an ideal soil; correction of formulas by W. B. Haines. *J. Agric. Sci.* **16**, 492–505.
- Fisher, L. R. & Israelachvili, J. (1981). Experimental studies on the applicability of the Kelvin equation to highly curved concave menisci. *J. Colloid Interface Sci.* **80**, No. 2, 528–541.
- Fisher, L. R. & Lark, P. D. (1980). The effect of adsorbed water vapour on liquid water flow in Pyrex glass capillary tubes. *J. Colloid Interface Sci.* **76**, No. 1, 251–253.
- Fitzpatrick, J. J., Iqbal, T., Delaney, C., Twomey, T. & Keogh, M. K. (2003). Effect of powder properties and storage conditions on the flowability of milk powders with different fat contents. *J. Food Engng* **64**, No. 4, 435–444.
- Fredlund, D. G. & Rahardjo, H. (1993). *Soil mechanics for unsaturated soils*. New York: Wiley.
- Gallipoli, D., Gens, A., Sharma, R. & Vaunat, J. (2003). An elastoplastic model for unsaturated soil including the effect of saturation degree on mechanical behaviour. *Géotechnique* **53**, 1, 123–135, <http://dx.doi.org/10.1680/geot.2003.53.1.123>.
- Gence, N. (2006). Wetting behavior of magnesite and dolomite surfaces. *App. Surf. Sci.* **252**, No. 10, 3744–3750.
- Hennig, A., Eichhorn, K.-J., Staudinger, U., Sahre, K., Rogalli, M., Stamm, M., Neumann, A. W. & Grundke, K. (2004). Contact angle hysteresis: study by dynamic cycling contact angle measurements and variable angle spectroscopic ellipsometry on polyimide. *Langmuir* **20**, No. 16, 6685–6691.
- Hoffman, R. L. (1975). A study of the advancing interface. I. Interface shape in liquid–gas systems. *J. Colloid Interface Sci.* **50**, No. 2, 228–241.
- Israelachvili, J. (1991). *Intermolecular and surface forces*, 2nd edn. London: Academic Press.
- Jaquin, P. A., Augarde, C. E., Gallipoli, D. & Toll, D. G. (2009). The strength of unstabilised rammed earth materials. *Géotechnique* **59**, No. 5, 487–490, <http://dx.doi.org/10.1680/geot.2007.00129>.
- Karagunduz, A., Pennell, K. D. & Young, M. H. (2001). Influence of a nonionic surfactant on the water retention properties of unsaturated soils. *Soil Sci. Soc. Am. J.* **65**, No. 5, 1392–1399.
- Lampenscherf, S., Pompe, W. & Wilkinson, D. S. (2000). Stress development due to capillary condensation in powder compacts: a two-dimensional model study. *J. Am. Ceram. Soc.*, **83**, No. 6, 1333–1340.
- Letley, J., Osborn, J. & Pelishek, R. E. (1962). Measurement of liquid–solid contact angles in soil and sand. *Soil Sci.* **93**, No. 3, 149–153.
- Lourenço, S. D. N., Gallipoli, D., Augarde, C., Toll, D., Evans, F. & Medero, G. (2008). Studies of unsaturated soils by environmental scanning electron microscope using dynamic mode. In *Unsaturated soils: Advances in geo-engineering* (eds D. G. Toll, C. E. Augarde, D. Gallipoli and S. J. Wheeler), pp. 145–150. Boca Raton, FL: CRC Press.
- Miller, C. R., Vogel, R., Surawski, P. P. T., Jack, K. S., Corrie, S. R. & Trau, M. (2005). Functionalized organosilica microspheres via a novel emulsion-based route. *Langmuir* **21**, No. 21, 9733–9740.
- Montes-H, G. (2005). Swelling–shrinkage measurements of bentonite using coupled environmental scanning electron microscopy and digital image analysis. *J. Colloid Interface Sci.* **284**, No. 1, 271–277.
- Reinson, J. R., Fredlund, D. G. & Wilson, G. W. (2005). Unsaturated flow in coarse porous media. *Can. Geotech. J.* **42**, No. 1, 252–262.
- Sjöblom, K. (2000). *The mechanisms involved during the desaturation process of a porous matrix*. PhD thesis, Massachusetts Institute of Technology, USA.
- Skauge, A., Spildo, K., Hoiland, L. & Vik, B. (2006). Theoretical and experimental evidence of different wettability classes. *J. Petrol. Sci. Engng* **57**, No. 3, 321–333.
- Sorgi, C. & De Gennaro, V. (2007). ESEM analysis of chalk microstructure submitted to hydromechanical loading. *C. R. Geosci.* **339**, No. 7, 468–481.
- Taniguchi, M. & Belfort, G. (2002). Correcting for surface roughness: advancing and receding contact angles. *Langmuir* **18**, No. 16, 6465–6467.
- Tuller, M., Or, D., Lynn, M. & Dudley, L. M. (1999). Adsorption and capillary condensation in porous media: liquid retention and interfacial configurations in angular pores. *Water Resour. Res.* **35**, No. 7, 1949–1964.
- Vaughan, P. R. & Walbancke, H. J. (1973). Pore pressure changes and delayed failure of cutting slopes in overconsolidated clay. *Géotechnique* **23**, No. 4, 531–539, <http://dx.doi.org/10.1680/geot.1973.23.4.531>.
- Weeks, B. L., Vaughan, M. W. & DeYoreo, J. J. (2005). Direct imaging of meniscus formation in atomic force microscopy using environmental scanning electron microscopy. *Langmuir* **21**, No. 18, 8096–8098.
- Wheeler, S. J., Sharma, R. S. & Buisson, M. S. R. (2003). Coupling of hydraulic hysteresis and stress–strain behaviour in unsaturated soils. *Géotechnique* **53**, No. 1, 41–54, <http://dx.doi.org/10.1680/geot.2003.53.1.41>.